Synthesis of Porous Palladium Superlattice Nanoballs and Nanowires

Hongkyu Kang, Young-wook Jun, Jong-Il Park, Kyung-Bok Lee, and Jinwoo Cheon*

Department of Chemistry and School of Molecular Science-BK21, Korea Advanced Institute of Science and Technology (KAIST), Taejon 305-701, Korea

Received July 26, 2000
Revised Manuscript Received September 29, 2000

Over the past decade, interest has grown in the synthesis of nanosized materials because of their novel electronic, optical, and catalytic properties.[1] Of the various methods available to prepare these materials, one of the most interesting is templated synthesis where the desired nanomaterial is encapsulated into the channels and pores of a host.[2] In particular, mesoporous solids with pore size tunability ranging from ≈2 to ≈30 nm have been the focus of special attention as hosts for quantum dots and wires.[3] For example, the pores of various mesoporous materials have been filled with polymers, semiconductors (CdS, GaAs, InP, GaN), metal oxides (Fe_2O_3), and metals (Ag, Pd, Pt) by either simple solution or vapor infiltration processes.[4] These processes, however, are often unable to fill the pores completely and sometimes generate undesired materials outside the host pores. In addition, the intimate contact between the host and guest can adversely affect the properties of the guest as has been observed for InP nanoparticles inside a zeolite.[5]

There are two important objectives in nanomaterials synthesis. First, it is advantageous to develop methods to synthesize nanoparticles free of the template hosts. Second, because the catalytic and physical properties of a nanoparticle strongly depend on its size and shape, it is important to devise methods that allow significant control over these morphological attributes. To date, only a few studies have achieved both of these goals in mesoporous template approaches: One of the studies used the two-step nanocasting process where mesoporous organic networks were grown by polymerization of monomers and subsequent removal of a silicate matrix.[6a,b] Excellent carbon-based mesoporous materials were also obtained from a MCM-48 template.[6c,d] As opposed to well-known inorganic oxides or ceramics, the fabrication of stable metallic structures with ordered nanopores of <10 nm are very rare and have only recently been realized for Ag, Pt, and Sn via the lyotropic liquid-crystalline approach.[7] Very recently, Stucky and co-workers reported the preparation of Au, Ag, and Pt nanowires using hexagonal mesoporous silica (SBA-15) via a solution-phase infiltration process.[8a] Ordered porous gold nanostructures with much larger pore dimensions (≈150 nm to 1 μm) have been synthesized by using latex spherical templates.[8b] In this regard, the development of a facile and reliable synthetic method for the ultra-small-scale metallic nanostructures is of particular interest.

In this communication, we present novel matrix free-palladium-based porous nanoballs and nanowires as well as palladium superlattices and wires inside of cubic MCM-48 and hexagonal SBA-15. To our knowledge, this report is the first to describe the syntheses of free-standing Pd nanostructures where the shape and size are precisely controlled with pore scales under 10 nm. Pd was chosen as the case study material because of its catalytic activity and its potential applications in H_2 storage and advanced electronics.[9]

Samples of granular MCM-48 (pore size of ≈3 nm) particles and SBA-15 (pore size of ≈9 nm) particles are dried at 400 °C for 8 h under a dynamic vacuum (≈10^{-2} Torr),[10] prior to introduction of the Pd metal-organic precursor, $Pd(hfac)_2$ (hfac = 1,1,1,5,5,5-hexafluoroacetylacetonate) via chemical vapor infiltration (CVI).[11] The precursor is sublimed into the empty pores of the mesoporous materials under vacuum at 55 °C; during this time the samples exhibit a color change from white to the yellow color indicative of the precursor.[12] The resulting $Pd(hfac)_2$@MCM-48 and $Pd(hfac)_2$@SBA-15

(1) See the reviews by (a) Schmid, G. *Chem. Rev.* **1992**, *92*, 1709. (b) Alivisatos, A. P. *J. Phys. Chem.* **1996**, *100*, 13226. (c) Alivisatos, A. P. *Science* **1996**, *271*, 933. (d) Steigerwald, M. L.; Brus, L. E. *Acc. Chem. Res.* **1990**, *23*, 183.

(2) (a) Martin, C. R. *Science* **1994**, *266*, 1961. (b) Martin. C. R. *Chem. Mater.* **1996**, *8*, 1739. (c) Kyotani, T.; Tsai, L.-F.; Tomita, A. *J. Chem. Soc., Chem. Commun.* **1997**, 701. (d) Routkevitch, D.; Bigion, T.; Moskovits, M.; Xu, J. M. *J. Phys. Chem.* **1996**, *100*, 14037. (e) Ozin, G. A.; Kuperman, A.; Stein, A. *Angew. Chem., Int. Ed. Engl.* **1989**, *28*, 359.

(3) (a) Kresge, C. T.; Leonowicz, M. E.; Roth, W. J.; Vartuli, J. C.; Beck, J. S. *Nature* **1992**, *359*, 710. See some reviews: (b) Zhao, D. Y.; Yang, P. D.; Huo, Q. S.; Chmelka, B. F.; Stucky, G. D. *Curr. Opin. Solid State Mater. Sci.* **1998**, *3*, 111. (c) Raman, N. K.; Anderson, M. T.; Brinker, C. J. *Chem. Mater.* **1996**, *8*, 1682. (d) Sayari, A. *Chem. Mater.* **1996**, *8*, 1840. (e) Ying, J. Y.; Mehnert, C. D.; Wong, M. S. *Angew. Chem., Int. Ed. Engl.* **1999**, *38*, 56. (f) Brinker, C. J. *Curr. Opin. Solid State Mater. Sci.* **1996**, *1*, 798. (g) Corma, A. *Chem. Rev.* **1997**, *97*, 2373.

(4) (a) Moller, K.; Bein, T. *Chem. Mater.* **1998**, *10*, 2950 and references therein. Some recent studies: (b) Srdanov, V. I.; Alxneit, I.; Stucky, G. D.; Reaves, C. M.; DenBaars, S. P. *J. Phys. Chem. B* **1998**, *102*, 3341. (c) Agger, J. R.; Anderson, M. W.; Pemble, M. E.; Terasaki, O.; Nozue, Y. *J. Phys. Chem. B* **1998**, *102*, 3345. (d) Winkler, H.; Birkner, A.; Hagen, V.; Wolf, I.; Fischer, R. A.; Schmechel, R.; Seggern, H. V. *Adv. Mater.* **1999**, *11*, 1444. (e) Wang, L.-Z.; Shi, J.-L.; Zhang, W.-H.; Ruan, M.-L.; Yu, J.; Yan, D. S. *Chem. Mater.* **1999**, *11*, 3015. (f) Mehnert, C. P.; Weaver, D. W.; Ying, J. Y. *J. Am. Chem. Soc.* **1998**, *120*, 12289. (g) Yamamoto, T.; Shido, T.; Inagaki, S.; Fukushima, Y.; Ichikawa, M. *J. Phys. Chem. B* **1998**, *102*, 3886.

(5) Trave, A.; Buda, F.; Fasolino, A. *Phys. Rev. Lett.* **1996**, *77*, 5405.

(6) (a) Johnson, S. A.; Ollivier, P. J.; Mallouk, T. E. *Science* **1999**, *283*, 963. (b) Göltner, C. G.; Weissenberger, M. C. *Acta Polym.* **1998**, *49*, 704. (c) Ryoo, R.; Joo, S. H.; Jun, S. *J. Phys. Chem. B* **1999**, *103*, 7743. (d) Lee, J.; Yoon, S.; Hyeon, T.; Oh, S. M.; Kim, K. B. *Chem. Commun.* **1999**, 2177.

(7) (a) Attard, G. S.; Bartlett, P. N.; Coleman, R. B.; Elliott, J. M.; Owen, J. R.; Wang, J. H. *Science* **1997**, *278*, 838. (b) Attard, G. S.; Göltner, C. G.; Corker, J. M.; Henke, S.; Templer, H. *Angew. Chem., Int. Ed. Engl.* **1997**, *36*, 1315. (c) Whitehead, A. H.; Elliott, J. M.; Owen J. R.; Attard, G. S. *Chem. Commun.* **1999**, 331.

(8) (a) Han, Y. J.; Kim, J.; Stucky, G. D. *Chem. Mater.* **2000**, *12*, 2068. (b) Velev, O. D.; Tessier, P. M.; Lenhoff, A. M.; Kaler, E. W. *Nature* **1999**, *401*, 548.

(9) *McGraw-Hill Concise Encyclopedia of Science and Technology*; Parker, S. P., Ed.; McGraw-Hill: New York, 1989; p 1343.

(10) The cubic MCM-48 and hexagonal SBA-15 hosts were prepared by a literature method. See: Zhao, D.; Feng, J.; Huo, Q.; Melosh, N.; Fredrickson, G. H.; Chmelka, B. F.; Stucky, G. D. *Science* **1998**, *279*, 548.

(11) $Pd(hfac)_2$ was synthesized following a literature method. See: Siedle, A. R.; Newmark, R. A.; Kruger, A. A.; Pignolet, L. H. *Inorg. Chem.* **1981**, *20*, 3399.

10.1021/cm000617f CCC: $19.00
Published on Web 11/11/2000

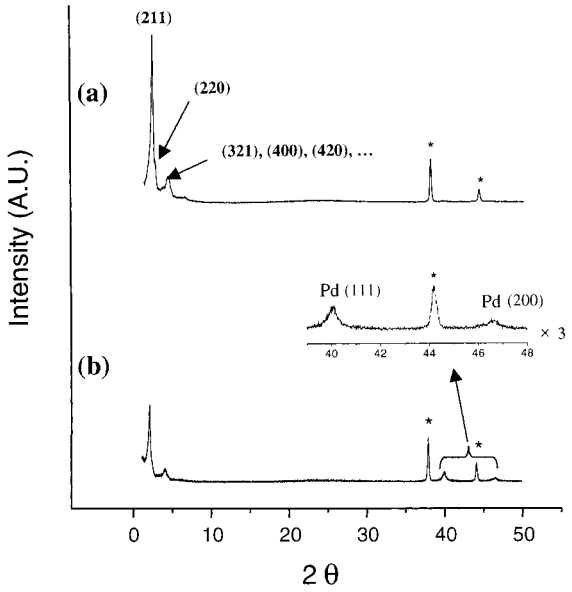

Figure 1. X-ray powder diffraction patterns: (a) peaks at low angles (1.2°−10°) are due to *Ia*3*d* symmetry of MCM-48; (b) Pd@MCM-48 formed by pyrolysis. Peaks due to the Al substrate are marked with asterisks.

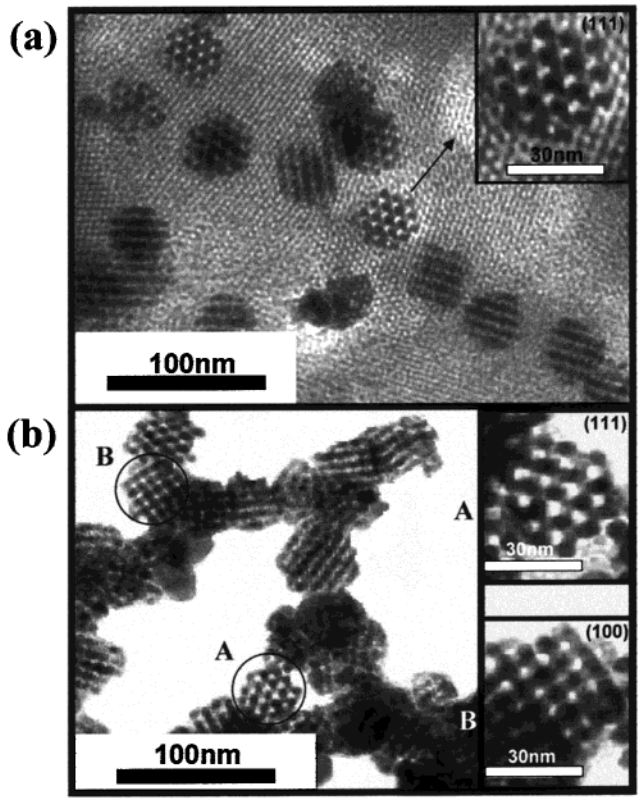

Figure 2. TEM images of (a) Pd@MCM-48 and (b) porous Pd superlattice nanoballs.

composites are then pyrolyzed at as low as 150 °C under a 10% H_2/N_2 flow to produce black powders of Pd@MCM-48 and Pd@SBA-15.

The X-ray diffraction patterns of MCM-48 and Pd@MCM-48 are shown in Figure 1.[13a] The low-angle peaks due to the silica matrix between 2θ values of 1.2° and 10° clearly show that major peaks corresponding to the *Ia*3*d* symmetry of the MCM-48 structure are observed throughout the process. Samples of the pyrolysis product Pd@MCM-48 exhibit two small broad diffraction peaks at 40.1° and 46.7° as a result of metallic Pd (Figure 1b).[13b,c] The significant decreases

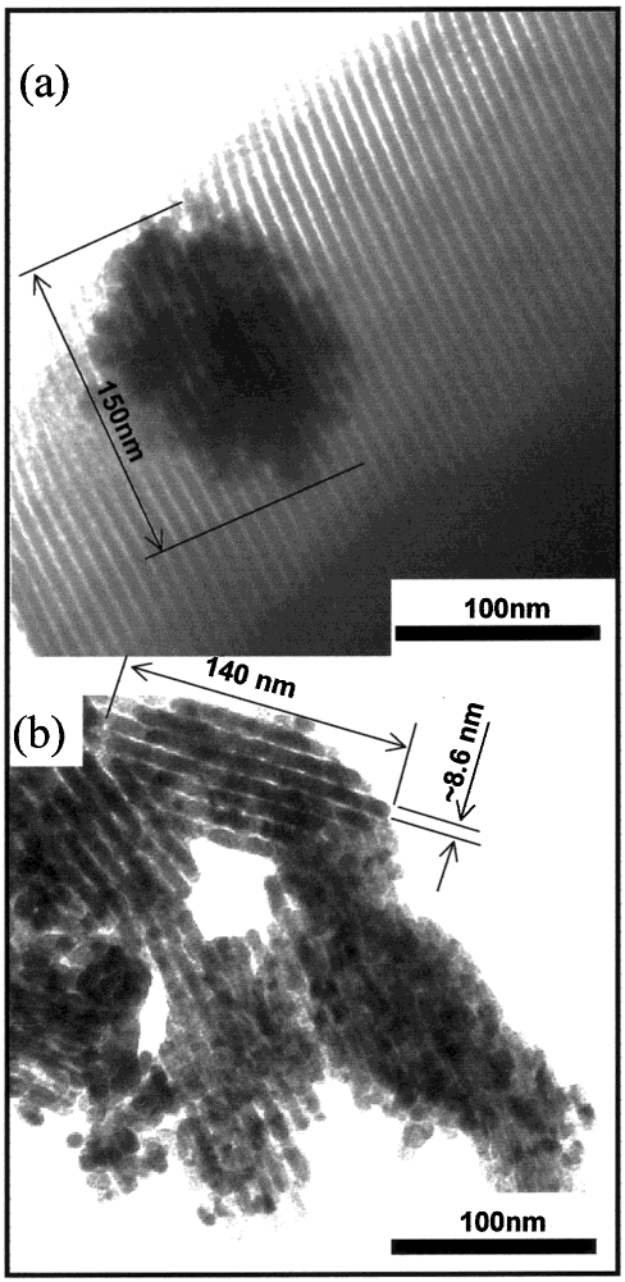

Figure 3. TEM images of (a) Pd@SBA-15 and (b) Pd nanowires.

(12) $Pd(hfac)_2$ is known to adsorb readily on silica surfaces by means of strong Lewis acid−base interactions between the Pd center and surface hydroxyl groups. See: Siedle, A. R.; Newmark, R. A. *J. Am. Chem. Soc.* **1981**, *103*, 1240.

(13) (a) X-ray diffraction patterns were collected on a Rigaku Miniflex (0.5 kW) diffractometer with Cu Kα radiation (λ = 0.1541 nm). Samples were placed on a 33-mm diameter aluminum holder. The diffraction angle was scanned from 1.12° to 50° with a 0.01° step width and a 0.01° s^{-1} scanning rate. (b) The Pd content was determined by ICP analysis on a Shimatzu ICPS-1000 III analyzer; the total Pd loading was found to be 6.0 wt % for Pd@MCM-48. (c) By this XRD analysis alone, it is not clear whether these peaks arise from Pd outside of the structure or inside the nanopores. (d) N_2 adsorption−desorption isotherms were measured at 77 K on a Micrometrics ASAP 2400 analyzer. (e) The pore structure of materials, and superlattices and nanowires, were observed on a EM 912 Omega TEM microscope operating at 120 kV with a point resolution of 3.7 Å.

in the intensities of the low-angle peaks due to the silica framework suggest that Pd has been encapsulated inside the pores.[14] BET measurements show that the surface areas and pore volumes decrease slightly:[13d] the surface areas decrease from 980 ± 4 m^2/g for MCM-48 to 937 ± 6 m^2/g for Pd@MCM-48, and the pore volumes decrease from 1.013 ± 0.004 cm^3/g for MCM-48 to 0.908 ± 0.006 cm^3/g for Pd@MCM-48. The relatively small changes indicate that the palladium is locally distributed inside the pores and do not block the channel entrances. These conclusions are supported by TEM analyses.[13e] For Pd@MCM-48, the TEM images show that the Pd aggregates into ball-shaped domains of 35−40 nm (average diameter = 38.2 nm, σ = 3.3); these domains consist of a three-dimensionally interconnected network of Pd-filled pores in the MCM-48 matrix of cubic *Ia*3*d* symmetry (Figure 2). Some pore-filled Pd nanoballs are clearly shown in the (111) crystallographic direction of the MCM-48 matrix (Figure 2a inset).[15] The formation of spherical ball-type domains can possibly be attributed to the mesoscale stress field of periodic mesoporous structures as similarly seen in the Ag system.[4e,16]

Careful treatment of Pd@MCM-48 with 20% HF dissolves the silicate matrix and affords a black powder suspension.[17] TEM examination of the powder shows that it consists of agglomerated and randomly stacked Pd nanoballs of 35−40 nm (average diameter = 37.6 nm, σ = 3.9). Each ball-shaped domain consists of a three-dimensionally interconnected network of Pd whose shapes and pores are obtained as the replication of the MCM-48 template (Figure 2b).[18] Some Pd nanoballs are clearly observed in the (111) and (100) crystallographic directions (Figure 2b inset). The structures of the Pd superlattices remain unchanged during the silicate dissolution process. Energy-dispersive X-ray emission analysis confirms that Pd is the major product without any significant contaminants.

The approach described above has been adopted to make Pd nanowires. The template used was hexagonal SBA-15, which has larger (≈9 nm diameter) straight channels. After CVI with $Pd(hfac)_2$ and pyrolysis of the resulting composite, Pd@SBA-15 is obtained. A TEM image (Figure 3a) shows that the Pd inside the channels is aggregated into large (≈150 nm) ellipsoidal domains consisting of a network of channel-filling Pd wires. Dissolving the silicate matrix in HF produces aggregates of Pd nanowires. The average diameter of each nanowire in the TEM image is about 8.6 nm (Figure 3b), which is nearly identical to the ≈9 nm channel diameter of the SBA-15 matrix. Presumably, the structure of the liberated Pd nanowires is dictated by the arrangement of channels in the SBA-15 template, although it is possible that the nanowires aggregate in this way simply to reduce the free surface energy.

In summary, arrays of palladium nanostructures have been obtained inside MCM-48 and SBA-15, using chemical vapor infiltration. Subsequent removal of the silica matrix with HF affords porous three-dimensional Pd nanoballs and one-dimensional Pd nanowires, depending on the architecture of the silicate host. These experiments constitute the first demonstration of shape- and size-controlled matrix free Pd nanostructures via a mesoporous template-assisted process. In particular, this low-temperature CVI approach, which should be applicable to other metals and mesoporous templates, is attractive because it can be carried out under conditions mild enough to avoid any disruption of both the desired material and the template structure. The approach makes possible the synthesis of various nanoporous and nanostructured materials, which may be technologically useful for catalytic, optoelectronic, and energy storage applications.

Acknowledgment. This work was supported by the Korea Research Foundation Grant (KRF-2000-015-DS0023). We thank Prof. R. Ryoo of KAIST for his kind helps in carrying out the research.

CM000617F

(14) Marler, B.; Oberhagemann, U.; Vortmann, S.; Gies, H. *Microporous Mater.* **1996**, *6*, 375.

(15) Alfredsson, V.; Anderson, M. W. *Chem. Mater.* **1996**, *8*, 1141.

(16) (a) Pohl, K.; Bartelt, M. C.; Figuera, J. de la; Bartelt, N. C.; Hrbek, J.; Hwang, R. Q. *Nature* **1999**, *397*, 238. (b) Zhang, Z. Y.; Lagally, M. G. *Science* **1997**, *276*, 377. (C) Conners, L.; Hollis, T.; Johnson, D. A.; Blyholder, G. *J. Phys. Chem. B* **1998**, *102*, 10112.

(17) HF is a very hazardous and corrosive chemical and should be handled according to the MSDS guidelines.

(18) The pore diameters are roughly estimated as 1.5−2.0 nm by HRTEM analysis and appear to be slightly bigger than the replica wall thickness (≈1.4 nm) of the MCM-48 templates.